SCCO: Thermodiffusion for the Oil and Gas Industry

Guillaume Galliero, Henri Bataller, Jean-Patrick Bazile, Joseph Diaz, Fabrizio Croccolo, Hai Hoang, Romain Vermorel, Pierre-Arnaud Artola, Bernard Rousseau, Velisa Vesovic, et al.

SCCO: Thermodiffusion for the Oil and Gas Industry

Guillaume Galliero, Henri Bataller, Jean-Patrick Bazile, Joseph Diaz, Fabrizio Croccolo, Hai Hoang, Romain Vermorel, Pierre-Arnaud Artola, Bernard Rousseau, Velisa Vesovic, Mounir Bou-Ali, José M. Ortiz de Zárate, Shenghua Xu, Ke Zhang, François Montel, Antonio Verga and Olivier Minster

Abstract The accurate knowledge of pre-exploitation fluid compositional profile is one of the necessary pre-requisites for a successful field plan development of a petroleum reservoir by the oil and gas industry. Thermodiffusion, leading to a partial diffusive separation of species in a mixture subject to thermal gradient, is thought to play an important role in oil and gas reservoir due to the geothermal gradient.

G. Galliero (✉) · H. Bataller · J.-P. Bazile · J. Diaz · F. Croccolo · H. Hoang · R. Vermorel · F. Montel
Laboratoire des Fluides Complexes et leurs Réservoirs - IPRA, UMR-5150 CNRS-TOTAL, E2S - Université de Pau et des Pays de l'Adour, Pau, France
e-mail: guillaume.galliero@univ-pau.fr

F. Croccolo
Centre National d'Etudes Spatiales (CNES), 2, Place Maurice Quentin, 75001 Paris, France

P.-A. Artola · B. Rousseau
Laboratoire de Chimie-Physique, UMR 8000, CNRS, Université Paris-Sud, Orsay, France

V. Vesovic
Department of Earth Science and Engineering, Imperial College London, London, UK

M. Bou-Ali
Mechanical and Industrial Manufacturing Department, Mondrago, MGEP Mondragon GoiEskola Politeknikoa, Arrasate, Spain

J. M. O. de Zárate
Departamento de Física Aplicada I, Universidad Complutense, Madrid, Spain

S. Xu
Key Laboratory of Microgravity (National Microgravity Laboratory), Institute of Mechanics, Chinese Academy of Sciences, No. 15 Beisihuanxi Road, Haidian District, Beijing 100190, China

K. Zhang
State Key Laboratory of Enhanced Oil Recovery (Research Institute of Petroleum Exploration & Development), CNPC, Beijing, China

F. Montel
TOTAL Exploration Production, Pau, France

A. Verga · O. Minster
European Space Agency, ESTEC, Noordwijk, The Netherlands

W. Hu and Q. Kang (eds.), *Physical Science Under Microgravity: Experiments on Board the SJ-10 Recoverable Satellite*, Research for Development,
https://doi.org/10.1007/978-981-13-1340-0_8

454183_1_En_8_Chapter ☑ TYPESET ☐ DISK ☐ LE ☑ CP Disp.:11/5/2019 Pages: 21 Layout: T1-Standard

Although major improvements in measuring, simulating and modelling thermodiffusion coefficients have been achieved in the last decades, the improvements are mostly limited to binary liquid mixtures at atmospheric pressure. Thus, the need for accurate data, that would prove invaluable as benchmark reference data for validating models and simulations, was one of the main drivers behind the project "Soret Coefficient measurements of Crude Oil" (SCCO) which used a microgravity set-up implemented in the SJ-10 satellite. This unique project, resulting from a partnership between European Space Agency and China's National Space Science Center enhanced by collaboration among academics from France, Spain, United Kingdom, China and industrialists from France and China, aimed to measure the thermodiffusion coefficients of multicomponent oil and gas mixtures under high pressures. Within this framework, some results on thermodiffusion of one ternary oil mixture and one quaternary gas condensate have been obtained in microgravity and have been qualitatively confirmed by molecular simulations. More precisely, these microgravity results have confirmed on multicomponent mixtures that thermodiffusion leads to a relative migration of the lightest hydrocarbon to the hot region. These results support the idea that, in oil and gas reservoirs, thermodiffusion is not negligible being able to counteract the influence of gravity-driven segregation on the vertical distribution of species.

Keywords Thermodiffusion · Segregation · Multicomponent mixtures · Oil and gas · Molecular dynamics

1 Introduction

The ever increasing world-wide energy demand is putting severe pressure on our ability to manage it effectively, while minimizing adverse climate effects. Although, the renewable energy sources are making strong in-roads, gas and oil remain an important part of the current and near-future energy landscape [1]. Natural gas and crude oil, the two most well-known examples of reservoir fluids, are found, in general, at depths greater than 500 m and require bringing to the surface in a controlled manner. Reservoir fluids, that reside within the pores of petroleum bearing rocks are the remnants of the transformation of organic matter (kerogen) over geological timescales. They are chemically complex mixtures consisting of hundreds of different species, primarily hydrocarbons. In order to optimally exploit the available resources, the petroleum industry creates a considerable demand for reliable values of the thermophysical properties of reservoir fluids over extensive ranges of temperature and pressure. The estimates of thermophysical properties of interest, mainly density and viscosity, can be obtained by a number of standard methods [2].

The petroleum reservoirs are typically subjected to external pressure and/or temperature fields so that gradients in chemical potentials are established leading to diffusive fluxes and resulting in a non-uniform compositional profile. Knowledge of such a profile, especially pre-exploitation profile, is one of the necessary

pre-requisites for a successful field plan development of a petroleum containing reservoir.

The non-uniform distribution of species in the reservoir is known to be influenced by a number of phenomena [3]; for instance, in a closed, convection-free reservoir gravitational segregation is assumed to be the most important [4]. However, if there is a temperature gradient within the reservoir, and most reservoir fluids are subject to at least a vertical geothermal gradient of about 0.03 K/m [3], the coupling of heat and mass fluxes [5] leads to a phenomenon known as thermodiffusion, which is also referred to as Soret effect. Thermodiffusion has been shown to strongly influence compositional distribution profile of species [3, 6, 7]. Indeed, there is some evidence based on a number of reservoirs, that thermodiffusion can be as important as gravitational segregation [6, 8–10].

In order to correctly model the thermodiffusion effects one needs a knowledge of thermodiffusion coefficients [5]. Although, there has been a major improvement in the accuracy and reliability in measuring thermodiffusion coefficients in the last decades [11, 12], the improvements are mostly limited to binary liquid mixtures at atmospheric pressure. Recently, the database of the available experimental data has been enhanced by new measurements on ternary mixtures [12, 13] and under high pressures [14–17]. As it is not possible to characterize all the relevant mixtures experimentally, a major effort has been undertaken to develop reliable prediction methods. Progress has been achieved both in the field of thermodiffusion simulation [18] and modelling [12]. Nevertheless, progress has been scant as far as the oil and gas at typical reservoir conditions are concerned, even when the reservoir fluids were represented by synthetic multicomponent mixtures consisting of a few species. The primary reason for this state of affairs can be traced to: (i) complexity of characterizing the thermodiffusion in multicomponent mixtures and (ii) the small magnitude of the thermodiffusion effect under normal laboratory conditions. The latter can be addressed by performing measurements under microgravity conditions [9, 19–22].

The need for accurate data, that can serve as benchmark reference data that would prove invaluable in validating models and simulations, was one of the main drivers behind the project “Soret Coefficient measurements of Crude Oil” (SCCO). The project aimed to measure the thermodiffusion coefficients of six multicomponent fluid mixtures, of interest to reservoir applications, under high pressures used a microgravity set-up implemented in the SJ-10 satellite [23]. The SCCO/SJ-10 project is the result of a unique partnership between the European Space Agency and China’s National Space Science Center [24] enhanced by collaboration among academics from France (Université de Pau et des Pays de l’Adour, Université de Paris-Sud and CNRS), Spain (Mondragon Unibertsitatea and Universidad Complutense), United Kingdom (Imperial College London), China (Chinese Academy of Sciences) and industrialists from France (TOTAL) and China (RIPED, CNPC).

In this chapter we aim to summarize some of the results of the project within a context of a short thermodiffusion review and make them available to the larger scientific community.

2 Quantifying Thermodiffusion

As already alluded to in the Introduction, a presence of temperature gradient within a convection-free fluid, generates a composition gradient in a mixture, that results in preferential migration of species towards either cold or hot sections. This separation effect occurs also when fluids are confined in a porous medium. It has been shown that the porous medium has a negligible effect on the magnitude of thermodiffusion, as long as one is not dealing with nano-pores [25]. Thus, the measurements of thermodiffusion coefficients in unconfined fluids can be used for most reservoir applications [26, 27].

The analysis of thermodiffusion is usually performed in the framework of non-equilibrium thermodynamics [5]. In this formalism, the macroscopic relation describing the transport of matter in a two-component mixture can be expressed as

$$\mathbf{J}_1 = -L_{1q}\frac{\nabla T}{T^2} - L_{11}\frac{\mu_{11}^w}{w_2 T}\nabla w_1 \tag{1}$$

where $\mathbf{J}_1$ is the mass flux of component 1, in a centre of mass reference frame, T is the temperature and μ_{11}^w is the derivative of the chemical potential of species 1 relative to its mass fraction, w_1. The L_{ij} are the so-called *phenomenological* or Onsager coefficients, describing the proportionality between fluxes and thermodynamic forces. At the stationary state, i.e. at null mass flux, the partial separation of the species induced by thermodiffusion in binary mixtures is usually quantified by the Soret coefficient, that is defined by,

$$S_T = -\frac{\nabla w_1}{w_1(1-w_1)\nabla T} = -\frac{\nabla x_1}{x_1(1-x_1)\nabla T} \tag{2}$$

where x_1 is the mole fraction of component 1. Note that with the definition given in Eq. (2) the value of the Soret coefficient for a binary mixture is independent of whether mass or molar concentrations are used. By combining Eqs. (1) and (2), an expression of the Soret coefficient in terms of the L_{ij}'s can be given,

$$S_T = -\left(\frac{1}{w_1\mu_{11}^w T}\frac{L_{1q}}{L_{11}}\right)_{\mathbf{J}_1=0} \tag{3}$$

In a multicomponent mixture, it is not possible to quantify thermodiffusion without specifying the reference frame. Although there is still some confusion in the literature, it is lately becoming more customary to quantify thermodiffusion in multicomponent mixtures by the so-called (molar) thermal diffusion ratio of each species, which is a dimensionless number defined by,

$$k_{T_i} = -T\frac{\nabla x_i}{\nabla T} \tag{4}$$

with temperature and composition gradients at steady state. The results of the SCCO microgravity experiment will be reported in terms of these (molar) thermal diffusion ratios.

Thermodiffusion has been extensively studied, in particular in binary liquid hydrocarbon mixtures, by experimental, modelling and simulation means. We present in the following a brief review of recent approaches, in particular those developed by the authors in connection with the SCCO project. The reader is referred to the literature for more comprehensive reviews [12, 18, 28, 29] on this topic.

2.1 *Experimental Investigations*

When a temperature gradient is applied to a fluid, because of thermal expansion, a density gradient appears. If the fluid is a mixture, the Soret effect will induce a compositional gradient which will modify this density gradient. Depending on the relative orientations of the density gradient and the gravity field, convection may occur in terrestrial laboratories. There are two families of experimental set-ups to measure the Soret effect: thermo-gravitational columns, which take advantage of convection, and Soret cells, which work only in a quiescent, purely conductive heat regime. In the framework of the SCCO project, measurements combining these two techniques have been recently performed on binary mixtures of *n*-alkanes under high pressure [16, 17].

2.1.1 Thermo-gravitational Columns

Following the ground-breaking experiments of Ludwig and Soret in U-shaped glass tubes, the invention of the Clusius–Dickel tube and its application to liquid mixtures [30] was an early milestone in the development of experimental devices capable of accurate and reliable thermodiffusion measurements. The evolution of these devices [31–33] has led to the method usually known as the Thermo-Gravitational Column (TGC) technique. A TGC consists of two vertical plates or concentric cylinders that are separated by a narrow gap, which contains the mixture, across which a temperature gradient ∇T is maintained perpendicular to gravity [34–36]. Coupling of thermodiffusion and solutal expansion induces thermo-solutal convection that highly amplifies the top-bottom gravitational separation. In this technique, it is the so-called thermodiffusion coefficient, D_{T}, which is directly measured. For a binary mixture, D_{T} is expressed as the product of the mutual diffusion coefficient D and the Soret coefficient (i.e. $D_T = S_T D$). The theory for concentric TGCs was originally developed by Furry, Jones and Onsager in 1939 [37] and its validity limits have been discussed, among others, by Valencia et al. [38].

TGCs have not only been used to measure thermodiffusion coefficients of binary mixtures of small molecules at normal and high pressures [14], but also for mixtures near the critical point [39]. More recently, the TGC technique has been extended to

ternary mixtures [40–43]. TGCs have also been filled with granular matter in order to study the Soret effect in porous media, and to model the separation mechanisms in situations more relevant for geochemical fluids [44, 45].

2.1.2 Soret Cells

A Soret cell is a sample volume bounded by two horizontal parallel plates with a high thermal conductivity, typically copper. The plates have a vertical (z-direction) spacing h and are kept at two different temperatures in order to generate a temperature gradient ∇T parallel to gravity. The volume is laterally confined by a material of low thermal conductivity, frequently glass thus allowing for optical observation in a direction perpendicular to the temperature gradient [11, 12] which facilitates some experimental techniques to measure thermodiffusion, like optical beam bending. In this kind of cells, Soret coefficients (as well as other properties) can also be measured by light scattering from non-equilibrium fluctuations, in which case optical windows in the bounding plates are needed for optical access parallel to the gradient. This approach was first demonstrated by Segre et al. [46] who investigated small-angle Rayleigh light scattering due to temperature and composition fluctuations in a toluene/n-hexane mixture subjected to a stationary temperature gradient.

According to fluctuating hydrodynamics [47, 48], the intensity of scattered light is proportional to $(\nabla T)^2/q^4$ and, hence, it increases very strongly for small scattering wave numbers q. The q^{-4} divergence at $q \to 0$ eventually saturates due to gravity and finite size effects [49–51]. Building on the investigation of non-equilibrium fluctuations in Soret cells, Croccolo et al. [52] have recently obtained Soret and diffusion coefficients of binary mixtures from dynamic shadowgraph experiments. This shadowgraph technique in Soret cells has been extended to high pressures by Giraudet et al. [15].

To apply the dynamic shadowgraph technique for ternary mixtures, theoretical extensions were undertaken. Ortiz de Zárate et al. [53] extended the theory of non-equilibrium concentration fluctuations spectra and their dynamics to micro-gravity conditions, but without accounting for confinement effects. The validation was performed by comparing with the experimental results for a mixture of tetralin/isobutylbenzene/n-dodecane under terrestrial conditions but at large wave vectors, where gravity and confinement effects are negligible [54]. More recently, and in the framework of the SCCO project, gravity has been included in the theory [55]. There are several ongoing experimental verifications in this respect. The incorporation of confinement effects into the theory is currently being developed [56].

2.2 *Modelling Developments*

In the low density limit it is possible, by means of kinetic theory, to link thermodiffusion to the intermolecular forces [57, 58]. However, and despite numerous efforts and

recent progress [12], there is still a lack of a universal microscopic picture explaining thermodiffusion in condensed phases. The lack of an underlying theory is quite general for transport properties [28], but for thermodiffusion it is compounded by its extreme sensitivity to molecular interactions, in particular to cross interactions [59].

When dealing with dense atomic and molecular fluids, there are basically three modelling approaches that have been proposed during the last century. The earliest ones are based on adaptations of the kinetic theory to dense phases [58, 60–62]. They were followed by ones based on pure equilibrium considerations of the phenomena [63] and subsequently by the ones based on liquid states theory [64–66]. There exist also some dedicated empirical approaches which lead to reasonable results when dealing with *n*-alkanes [59, 61, 67].

In the oil and gas industry, the most popular models are probably those based on equilibrium concepts as they can be linked with thermodynamics quantities readily available in most PVT software packages that make use of Equations of States (EoS). This is somewhat surprising as it is known that such models are not very accurate because of their sensitivity to the choice of the EoS, as thermodiffusion quantification requires second derivatives of thermodynamic properties [68]. Furthermore, these equilibrium type models do not account correctly for the contribution due to irreversibility, although this is not the dominant term in quasi-ideal mixtures, like petroleum fluids [28]. In addition, equilibrium type models cannot take into account properly the mass difference ("isotope") effect which is well correlated with the Soret coefficient in simple linear alkanes [67, 69].

At present, the most promising thermodiffusion models to apply to petroleum fluids are probably those of Artola et al. [64] and of Würger [66] that contain contributions from both equilibrium and irreversibility (through terms related to the mobility of the species). However, these two models still need to be tested systematically against the available data on binary mixtures, in order to better understand how the mobility is related to molecular parameters and thermodynamic conditions. In addition, these models need to be extended to multicomponent mixtures [70], so that they can be applied to real petroleum fluids.

2.3 *Molecular Simulations*

Equations (2) and (3) offer two different routes to compute the Soret coefficient in binary mixtures by means of molecular dynamics simulations. In approaches using Eq. (2), one mimics a real experiment by introducing a thermal gradient or by imposing a heat flux in the simulation box. Such methods are classified as "boundary driven non-equilibrium molecular dynamics" (BD-NEMD) methods [71, 72].

The other route, through Eq. (3), consists in directly computing the Onsager coefficients L_{ij} either by using equilibrium molecular dynamics (EMD) and the Green-Kubo formalism [73], or by the synthetic non-equilibrium molecular dynamics (S-NEMD) algorithms proposed by Evans [74, 75] or Ciccotti [76]. One drawback in the determination of S_T through the computation of L_{ij} is that additional quantities

are needed to relate the L_{ij} to the experimentally accessible S_T, namely, the value of the thermodynamic factor μ_{11}^w. For isotopic or nearly ideal mixtures, one can use the ideal value of μ_{11}^w as a first approximation. However, for a non-ideal mixture, μ_{11}^w differs from the ideal value, strongly affecting the final value of the Soret coefficient. Additional thermodynamic quantities also appear in the expression of L_{1q}, since in the case of mixtures the heat flux J_q is not directly accessible by molecular simulation. In particular, one needs the values of the partial enthalpies of the different components to compute L_{1q} [76]. Therefore, BD-NEMD methods which provide directly Soret coefficients (and thermal diffusion ratios) are becoming the main methods used to obtain the Soret coefficient for realistic mixtures.

Molecular simulation of thermodiffusion has long been limited to the simplest models, i.e. binary Lennard-Jones mixtures. As a result of advances in parallel computing and adapted molecular dynamics simulation packages, it has now become possible to produce quantitative predictions using realistic molecular models, of interest to the crude oil industry. Simon et al. [77] and more recently Antoun et al. [78] employed BD-NEMD to compute the Soret coefficients in alkane binary mixtures. Perronace et al. [79] performed an extensive study of Soret coefficients in *n*-pentane–*n*-decane mixtures using EMD, S-NEMD and BD-NEMD simulations. Their results were compared to experimental data and gave a satisfactory agreement. Zhang and Müller-Plathe [80] applied BD-NEMD method to investigate thermodiffusion in benzene–cyclohexane mixtures at three different compositions. In a series of articles, Polyakov and colleagues [81, 82] studied the behaviour of alkane/aromatic mixtures in which they show that the Soret coefficient becomes larger with increasing the degree of branching of the hydrocarbon, thus confirming the experimental findings. Recently and in the context of the SCCO project, molecular simulations have been used to study thermodiffusion in non-binary mixtures [70, 83], as well as in coupling thermodiffusion with gravity segregation so as to mimic the behaviour of a one-dimensional reservoir [9, 10].

3 The SCCO-SJ10 Experiment

The experimental set-up flown in SJ-10 consists of six small and sturdy titanium cells developed for ESA by *Core Laboratories: Sanchez Technologies* (Paris, France) and designed to operate at high pressures (HP). These HP cells are built by screwing two titanium end parts to an initially open motorized cylindrical rotating ball valve which, when closed, divides the inner volume into two exactly equal halves. The dimensions of the inner cylinder of the HP cells are: a total length of L = 40 mm and a diameter of D = 6 mm, which becomes a bit narrower in the channel that crosses the ball of the valve, resulting in a total volume of about 1.2 mL. Kalrez 6375 O-ring were selected as sealing materials for the titanium end parts and for the valve sealing stack. HP cells have been certified for pressures up to 600 bars. For temperature control, two aluminium blocks are attached (screwed) at the titanium end parts. Figure 1 shows one of the SJ10-SCCO cells before integration. A cross-section schematic representation

Fig. 1 One of the HP cells flown in SJ10 before integration in its triad and in the C-Box. Note the two aluminium blocks attached at the titanium end parts

of an individual cell can be found in Ref. [23]. Electrical heaters are placed at the two end aluminium blocks and the HP cells, thus fashioned, are attached to two supporting triads and integrated into a hermetically sealed aluminium crate, named C-box, see Fig. 2, which also contains the electronics for temperature control and communications. During the orbital flight the two aluminium blocks of every HP cell were maintained at different temperatures, so as to induce thermodiffusion inside the fluid contained therein. Pt100 sensors with accuracy standard uncertainty of 0.05 K placed at the two ends of each HP cell are used to monitor temperatures through the duration of the experiment. Time-stamped temperature readings are stored in a flash disk also contained in the C-Box. At the end of the experiment the central valves in all HP cells were closed shut separating each fluid sample into two fractions (a "hot" and a "cold" part), which, once recovered after re-entry, were forwarded to the State Key Laboratory of Enhanced Oil Recovery (Research Institute of Petroleum Exploration & Development) for composition analysis. The set-up is similar to the one used during the Foton-M3 mission in 2007 and further details can be found elsewhere [9, 21].

As already described [23] the SCCO-SJ10 experiment has been conducted on six different synthetic mixtures that contain hydrocarbons found in reservoir fluids. The samples were composed of linear alkanes: methane (C1), *n*-pentane (nC5), *n*-heptane (nC7) and *n*-decane (nC10). Binary, ternary and quaternary mixtures containing the aforementioned species have been studied under high pressure in a monophasic state.

Fig. 2 Left: The six HP cells contained in the C-box. Right: The C-box once closed

Table 1 summarizes the composition and pressures used in the six different experimental HP cells. Pressures correspond to the in-flight average temperature of 50.8 °C at which experiments were performed, as further elucidated in Sect. 2 of Chap. 3. The fluids in HP cells A–D are in a compressed liquid state, while HP cells E and F contain compressed gas, which on lowering the pressure produces a small amount of liquid. The latter mimics an important class of fluids of interest to the oil and gas industry, namely gas condensate, which is monophasic in reservoir conditions but diphasic (gas + "condensate", i.e. liquid) at atmospheric conditions. Preparation and injection of the fluids mixture inside the HP cells have been performed in the State Key Laboratory of Enhanced Oil Recovery of the Research Institute of Petroleum Exploration & Development in Beijing as described in Sect. 1 of Chap. 3.

On April 6th at 01:38 local time, a Long March (Chang Zheng) 2D rocket lifted-off from China's Jiuquan Satellite Launch Centre carrying the SJ-10 (Shi Jian 10) research spacecraft. The satellite's scientific payload entailed of a variety of experiments including SCCO. SJ-10 landed on April 18th at 15:04, approximately 12.5 days after its launch, in the Inner Mongolia region north of Beijing. The SCCO C-Box was transported, within a day, to the State Key Laboratory of Enhanced Oil Recovery in Beijing. Additional technical details of the mission are provided in the sections below.

Table 1 Composition and pressure of the six SCCO HP cells embarked in SJ10 (adapted from Ref. [23])

HP cell	Pressure (MPa)	Composition (mole fraction)			
		C1	nC5	nC7	nC10
A	31.1	–	0.5	–	0.5
B	40.2	–	0.5	–	0.5
C	31.0	–	0.3333	0.3333	0.3334
D	40.1	–	0.3333	0.3333	0.3334
E	35.0	0.9649	0.0117	0.0117	0.0117
F	40.0	0.9649	0.0117	0.0117	0.0117

3.1 *Fluid Preparation and HP Cell Filling Process*

The experiments were performed at pressures given in Table 1 and at the flight operating average temperature of 50.8 °C [23]. In order to achieve these conditions, the HP cells were filled on the ground at 20 °C under a filling pressure that corresponds to the target pressure for each HP cell at the flight operating temperature. The required filling pressure was estimated by means of a Peng-Robinson equation of state [84], as the design of SCCO did not allow for pressure sensors inside the HP cells. Three STIGMA automatic pumps from Core Laboratories were used for sample preparation and HP cell filling procedures. Each pump controlled the injection pressure, the injected volume and temperature. Two different protocols [23], further described below, have been used depending on the mixture type, see Fig. 3.

3.1.1 Binary and Ternary (Liquid) Mixtures Preparation

The four liquid mixtures (A–D) were prepared by first introducing nC5 into pump 1, see Fig. 3 Then, the pre-evacuated pump 2 was filled with, either nC10 or with a nC7–nC10 premix by aspiration and weight control. The desired amount of nC5 was introduced into pump 2 from pump 1 and the mixtures were homogenized by integrated mechanical stirring and then injected into the SCCO HP cells. The cell volume was swept at least three times by the sample. The HP cell pressure was adjusted and controlled by pump 2.

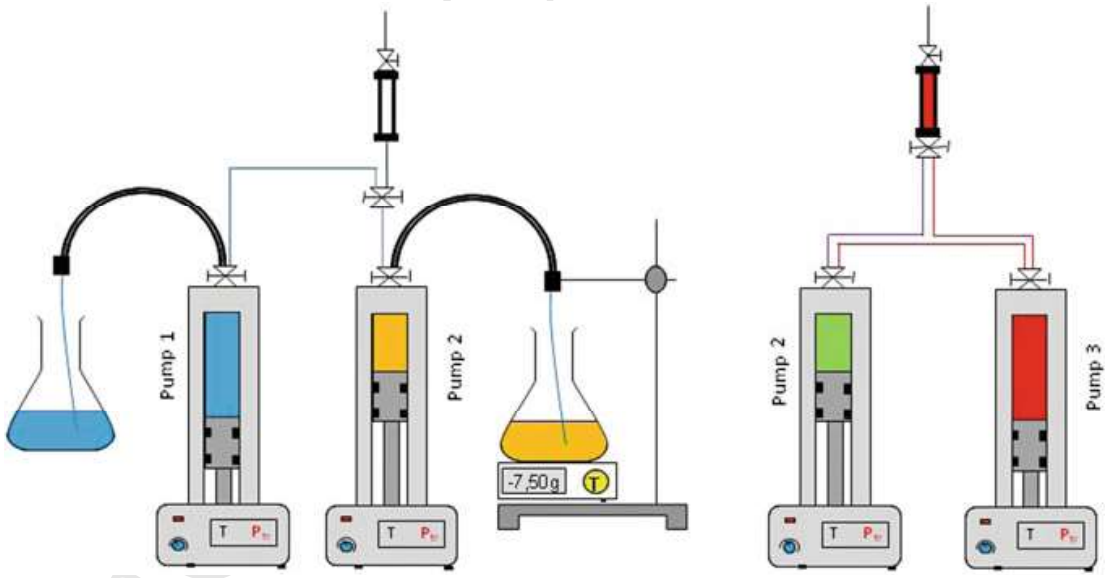

Fig. 3 Sketches of the protocol for the liquid mixture preparation (left figure) and gas-liquid mixtures (right figure) (adapted from Ref. [23])

Table 2 Average temperatures on the cold and hot plates during operational time of 270 h

HP cell ID	T cold side (°C)	T hot side (°C)
A	35.85	65.88
B	35.86	65.88
C	35.84	65.88
D	35.83	65.88
E	35.85	65.88
F	35.87	65.88

3.1.2 Quaternary Mixture (Gas Condensate) Preparation and Filling

The quaternary mixtures of HP cells E and F are single phase at the operating temperature and pressures of Table 1. However, at the filling temperature of 20 °C and corresponding filling pressures they are phase-separated. Hence, it is not possible to use the protocol described in Sect. 3.1.1 and a new protocol was designed. The SCCO HP cells were initially filled with methane (C1) at 20 MPa. The pump 2 was then filled with a C5–nC7–nC10 equimolar ternary mixture using the same procedure as described above, while pure methane was introduced into pump 3 at a pressure of 27.5 MPa. Then, from pump 3 the desired quantity of methane was transferred into pump 2. The quaternary mixture so obtained was homogenized and pressurized to 27.5 MPa and then transferred into the HP cells. The HP cells volume was swept at least five times by the sample. The HP cells pressure was adjusted and controlled by pump 2.

3.2 Conditions During the SJ-10 Orbital Flight

The SCCO experiment was powered on after SJ-10 reached its stabilized orbit, on April 7th at exactly 14:00. The segregation of chemical species occurred in a controlled environment where smooth and seldom orbital manoeuvres resulted in only very small residual accelerations. Inside the C-box, a set of heaters (one per HP cell) and Peltier's (one per triad) elements maintained a relatively stable temperature difference between approximately 36 and 66 °C at each of the six samples. After activation and the initial transitory phase, the target temperatures at the two triads were met in about 40 min. Actual temperatures measured at the HP cell sides are displayed in Fig. 4, illustrating that during the remaining operational time, about 270 h long, the temperatures at the hot and cold sides of each high pressure HP cell were stable to within ±0.05 K. Average values of the temperatures measured at each side of the HP cells, after the short transient, are provided in Table 2.

Tightly attached to its SJ-10 cold plate, the C-Box containing the 6 HP cells kept a rather constant temperature of about 21 °C for the whole experimental run; it decreased to about 19 °C at the end of the orbital flight (see purple curves in

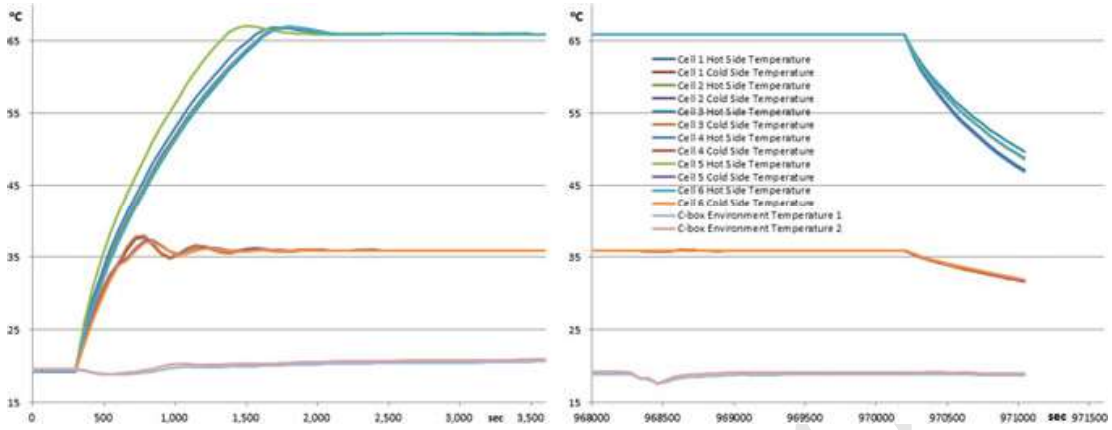

Fig. 4 Evolution of the temperature at the extremities of each HP cell, initial transient (left figure) and final transient (right figure)

Fig. 4). The C-Box is air tight and its inner pressure was continuously monitored. After a short, initial transient the pressure stayed at a relatively constant value of 1.18 ± 0.05 bar.

On April 17th at 21:09, the temperature control at two extremities of the six HP cells was automatically switched-off, following the closure of the intercepting valves about 12 min earlier. The subsequent slow decrease in temperature at both extremities of the HP cells observed in Fig. 4, had no effect on the mixture composition as the fluids remained safely confined within the two separate halves of the HP cells. Typical diffusion coefficients in this kind of hydrocarbon mixtures are at least of the order of 10^{-6} cm^2 s^{-1} [17], which combined with a HP cell length $L = 4$ cm gives a maximum experimental characteristic time, $\tau_{\max}$, of about 2.5×10^5 s. The duration of the runs, about $4\tau_{\max}$, is so considered long enough for the separation inside the six HP cells to have attained steady state. Twenty-four hours after capsule recovery, the SCCO C-Box was brought back to the State Key Laboratory of Enhanced Oil Recovery in Beijing, where engineers and scientists were ready to split it apart and reach the valuable flown samples of alkane mixtures, in order to start the gamut of tasks for their post-fight sample analysis.

3.3 High Pressure Cell Analysis Process

Two Agilent Gas Chromatographs (GC) 6890 N with Agilent 19091Z-205 HP-1 columns have been used to analyse the six samples; depending on the nature of the mixtures, two different protocols, as described previously [23], have been used.

3.3.1 Binary and Ternary Mixtures

For binary and ternary liquid mixtures (A–D) the HP cells were initially stored, at the CNPC laboratory, at −15 °C in order to limit evaporation of the lightest alkane (nC5). Following this pre-conditioning, the two compartments of each HP cell were emptied using dedicated syringes and the extracted fluids were then stored in Agilent vials with volume redactor. When the extracted volume was insufficient, the liquid samples were diluted in a solvent (carbon disulphide) which did not affect the analysis. Finally, the fluid samples were injected in the gas chromatograph and analysed.

3.3.2 Quaternary Mixtures

For quaternary gas condensate mixtures (E and F) the fluids contained in the two compartments of each HP cell, were initially diluted by using hydrogen, as to avoid phase separation. The resulting diluted mixtures were stored in a dedicated reservoir with a volume of 1 litre and subsequently transferred to the GC for analysis. The reservoirs were heated to the same temperature as the GC line, in order to avoid cold points.

3.4 Results and Discussions

From the gas chromatography analysis of all cold and hot compartments of each HP cell performed after the flight using the protocols above, it appeared that some HP cells have suffered from leakages yielding incoherent results. This conclusion is confirmed independently by accurate weighing of filled HP cells before and after the flight. The leakage may have many root causes, but most of them can be attributed to either unpredictable thermal effects at such high pressures inside the HP cells (more than 300 bar, See Table 1) or to unexpected landing shocks. In particular, HP cells A, B, D and F were found to be partially empty, to the extent that no sensible analysis could be performed and therefore they will not be discussed further. Results on the two exploitable HP cells (C and E), which contained a ternary and a quaternary mixture respectively, which have been presented previously [23], are displayed here in Table 3, for completeness and ease of discussion. The reported compositions in Table 3 have been estimated using normalized peaks-area computation and are an average between two different GC injections for each compartment. The associated error bars correspond to half the difference between the results of the two injections. The composition results were reproducible to within 2% of mole fraction of a given compound. It should be pointed out that the GC protocol has been tested on a HP cell that stayed on earth and was containing the same quaternary mixture as HP cells E and F.

Table 3 Measured GC compositions (in mole fraction) in the two exploitable HP cells after the flight. Initial compositions (before the flight) are shown in Table 1 (adapted from Ref. [23])

HP cell ID	Cold compartment				Hot compartment			
Species	C1	nC5	nC7	nC10	C1	nC5	nC7	nC10
C	N/A[a]	0.3063 ± 0.0151	0.333 ± 0.0033	0.3607 ± 0.0185	N/A[a]	0.3585 ± 0.0019	0.3337 ± 0.0025	0.3078 ± 0.0043
E	0.9612 ± 0.0007	0.0117 ± 0.0002	0.0138 ± 0.0001	0.0135 ± 0.0008	0.0969 ± 0.0056	0.0116 ± 0.0003	0.0096 ± 0.0004	0.0098 ± 0.0049

[a]N/A: Not applicable (Ternary mixture)

As shown in Table 3, compositions of the two compartments (cold and hot) of each exploitable HP cell are noticeably different, as expected. Furthermore, results clearly show that, in both liquid (HP cell C) and gas condensate (HP cell E) mixtures, the lightest species had a tendency to migrate (relatively to the heaviest) to the hot compartment, while the heaviest migrated towards the cold end. Such behaviour is consistent with what has been known qualitatively for a long time [85] and also with more recent experimental results on binary hydrocarbon mixtures [11, 12]. In addition, it appears that the intermediate species, nC7 in the ternary mixture and nC5 in the quaternary mixture, is uniformly distributed showing only weakly migrating patterns. Such a trend is also consistent with what is known regarding mass effect in non-binary mixtures [69, 70]. The observed behaviour is also in agreement with molecular dynamics results on multicomponent hydrocarbon mixtures [9, 10, 58]. More generally, these results confirm that, in oil and gas reservoirs composed of normal alkanes, thermodiffusion tends to counteract (and sometimes overcome) the influence of gravity-driven segregation on the vertical distribution of species [10].

From the compositional difference between the two compartments, and assuming a linear response, it is possible to quantify thermodiffusion in the studied mixtures by means of Eq. (4). Such a computation requires an estimation of the average temperature difference between the two compartments of each HP cell and following the work of Van Vaerenbergh [21], we estimated it to be equal to 12.45 ± 0.20 °C [23]. As explained above, it is also implicitly assumed that the duration of the experiment (270 h) is long enough for the stationary state to be reached. Results, presented in terms of the thermal diffusion ratio, are provided in Table 4.

Experimental values of thermal diffusion ratios shown in Table 4, confirm quantitatively what is observed in terms of the compositional variations of the cold and hot compartments, i.e. thermodiffusion leads to a relative migration to the hot region of the lightest hydrocarbon in a given mixture. What is more surprising is the magnitude of the thermal diffusion factors [23]. The values obtained for the quaternary mixtures, whose order of magnitude (about 0.1) is consistent with experimental results on non-polar binary mixtures [11, 12]. However, the thermal diffusion ratios for nC5

Table 4 Experimental measurements and molecular simulations results of thermal diffusion ratio of the various species in the two exploitable HP cells (adapted from Ref. [23])

HP cell ID	Thermal diffusion ratio per species (k_{T_i})							
	Experiments				Molecular simulations			
Species	C1	nC5	nC7	nC10	C1	nC5	nC7	nC10
C	–	−1.36 ± 0.47	−0.02 ± 0.14	1.38 ± 0.62	–	−0.09 ± 0.03	−0.09 ± 0.03	0.18 ± 0.04
E	−0.21 ± 0.17	0 ± 0.01	0.11 ± 0.09	0.1 ± 0.08	−0.16 ± 0.04	0.04 ± 0.01	0.05 ± 0.01	0.07 ± 0.02

and nC10 in the ternary liquid mixtures are one order of magnitude larger than those of the quaternary mixture.

To complement these microgravity experiments Boundary Driven Non Equilibrium Molecular Dynamics computations of the thermal diffusion ratios of HP cells C and E fluids have been performed using Mie Chain Coarse Grained molecular models to represent the fluid molecules [86]. Simulations details can be found in Ref. [23].

Simulations results, provided in Table 4, confirm what has been pointed out previously, i.e. microgravity experimental results on the ternary mixture are qualitatively consistent, but quantitatively questionable, whereas experimental results on the quaternary mixture are quantitatively consistent with molecular simulations results, reinforcing thus their reliability.

Dedicated on ground experiments and additional molecular simulations are in progress in order to further analyse these very interesting experimental results obtained in the microgravity environment of a space flight.

Acknowledgements This work has been supported by ESA's Microgravity Applications Programme through the SCCO project. The whole team warmly acknowledges the contributions of QinetiQ Space (Antwerp, Belgium), Core Laboratories: Sanchez Technology (Paris, France) and SISET (Yantai, China) for developing and building both hardware and software of the microgravity experimental set-up flown on SJ-10. The authors also thank TOTAL S.A. and PETROCHINA for permission to publish present and past data. The Spanish teams (Mondragon Unibertsitatea and Universidad Complutense) are thankful to the ATNEMFLU (ESP2017-83544-C3-1-P and ESP2017-83544-C3-2-P) of MINECO. HB and FC acknowledge financial support from the Centre National d'Etudes Spatiales (CNES). The Chinese teams acknowledge financial support from the National Natural Science Foundation of China (Grant No. U1738108) and foundation of SJ-10 recoverable satellite.

References

1. International Energy Outlook (IEO) (2017). www.eia.gov/outlooks/ieo/pdf/0484(2017).pdf
2. Danesh A (1998) PVT and phase behaviour of petroleum reservoir fluids. Elsevier Science, The Netherlands
3. Montel F, Bickert J, Lagisquet A, Galliero G (2007) Initial state of petroleum reservoirs: a comprehensive approach. J Pet Sci Eng 58:391–402

4. Sage BH, Lacey WN (1939) Gravitational concentration gradients in static columns of hydrocarbons fluids. Petr Trans AIME 132:120
5. de Groot SR, Mazur P (1984) Nonequilibrium thermodynamics. Dover, New York
6. Holt T, Lindeberg E, Ratkje KS (1983) The effect of gravity and temperature gradients on methane distribution in oil reservoirs, SPE Paper 11761
7. Whitson CH, Belery P (1994) Compositional gradients in petroleum reservoirs, SPE Paper 28000
8. Ghorayeb K, Firoozabadi A, Anraku T (2003) Interpretation of the unusual fluid distribution in the Yufutsu gas-condensate field. SPE J 8:114–123
9. Touzet M, Galliero G, Lazzeri V, Saghir MZ, Montel F, Legros JC (2011) Thermodiffusion: from microgravity experiments to the initial state of petroleum reservoirs. Comptes Rendus - Mécanique 339:318–323
10. Galliero G, Bataller H, Croccolo F, Vermorel R, Artola PA, Rousseau B, Vesovic V, Bou-Ali M, de Zarate JMO, Xu S, Zhang K, Montel F (2016) Impact of thermodiffusion on the initial vertical distribution of species in hydrocarbon reservoirs. Microgravity Sci Technol 28:79
11. Wiegand S (2004) Thermal diffusion in liquid mixtures and polymer solutions. J Phys: Cond Matter 16:R357–R379
12. Köhler W, Morozov KI (2016) The Soret effect in liquid mixtures—a review. J Non-Equilib Thermodyn 41:151
13. Bou-Ali MM, Ahadi A, Alonso de Mezquia D, Galand Q, Gebhardt M, Khlybov O, Köhler W, Larrañaga M, Legros JC, Lyubimova T, Mialdun A, Ryzhkov I, Saghir MZ, Shevtsova V, Van Vaerenbergh S (2015) Benchmark values for the Soret, thermodiffusion and molecular diffusion coefficients of the ternary mixture tetralin+isobutylbenzene+n-dodecane with 0.8-0.1-0.1 mass fraction. Eur Phys J E 38:30
14. Urteaga P, Bou-Ali MM, Alonso de Mezquía D, Santamaría J, Santamaría C, Madariaga JA, Bataller H (2012) Measurement of thermodiffusion coefficient of hydrocarbon binary mixtures under pressure with the thermogravitational technique. Rev Sci Instrum 83:074903
15. Giraudet C, Bataller H, Croccolo F (2014) High-pressure mass transport properties measured by dynamic near-field scattering of non-equilibrium fluctuations. Eur Phys J E 37:107
16. Lizarraga I, Giraudet C, Croccolo F, Bou-Ali MM, Bataller H (2016) Mass diffusion and thermal diffusivity of the decane-pentane mixture under high pressure as a ground-based study for SCCO project. Micrograv Sci Technol 28:267
17. Lizarraga I, Croccolo F, Bataller H, Bou-Ali MM (2017) Soret coefficient of the dodecane–hexane binary mixture under high pressure. Eur Phys J E 40:36
18. Artola PA, Rousseau B (2013) Thermal diffusion in simple liquid mixtures: what have we learnt from molecular dynamics simulations? Molec Phys 111:3394–3403
19. Legros JC, Van Vaerenbergh S, Decroly Y, Montel F (1994) Expériences en microgravité étudiant l'effet Soret: SCM, SCCO et MBIS, Entropie 198/199:1
20. Georis P, Montel F, Van Vaerenbergh S, Decoly Y, Legros JC (1998) Proc Eur Pet Conf 1:57–62
21. Van Vaerenbergh S, Srinivasan S, Saghir MZ (2009) Thermodiffusion in multicomponent hydrocarbon mixtures: experimental investigations and computational analysis. J Chem Phys 131:114505
22. Khlybov OA, Ryzhkov II, Lyubimova TP (2015) Contribution to the benchmark for ternary mixtures: measurement of diffusion and Soret coefficients in 1,2,3,4-tetrahydronaphthalene, isobutylbenzene, and dodecane onboard the ISS. Eur Phys J E 38:29
23. Galliero G, Bataller H, Bazile JP, Diaz J, Croccolo F, Hoang H, Vermorel R, Artola PA, Rousseau B, Vesovic V, Bou-Ali M, de Zarate JMO, Xu S, Zhang K, Montel F, Verga A, Minster O (2017) Thermodiffusion in multicomponent n-alkane mixtures. NPJ Microgravity 3:20
24. Hu WR, Zhao JF, Long M, Zhang XW, Liu QS, Hou MY, Kang Q, Wang YR, Xu SH, Kong WJ, Zhang H, Wang SF, Sun YQ, Hang HY, Huang YP, Cai WM, Zhao Y, Dai JW, Zheng HQ, Duan EK, Wang JF (2014) Space program SJ10 of microgravity research. Microgravity Sci Technol 26:156–169
25. Hannaoui R, Galliero G, Hoang H, Boned C (2013) Influence of confinement on thermodiffusion. J Chem Phys 139:114704

26. Shapiro A, Stenby EH (2000) Factorization of transport coefficients in macroporous media. Transp Porous Media 41:305–323
27. Platten JK, Costesèque P (2004) The Soret coefficient in porous media. J Porous Media 7:317–329
28. Assael MJ, Goodwin ARH, Vesovic V, Wakeham WA (2014) Experimental thermodynamics volume IX: advances in transport properties of fluids. Royal Society of Chemistry, London
29. Rahman MA, Saghir MZ (2014) Thermodiffusion or Soret effect: historical review. Int J Heat Mass Transf 73:693
30. Clusius K, Dickel G (1939) Das Trennrohrverfahren bei Flüssigkeiten. Naturwissenschaften 27:148
31. Jones RC, Furry WH (1946) The separation of isotopes by thermal diffusion. Rev Mod Phys 18(2):151–224
32. Majumdar SD (1951) The theory of the separation of isotope by thermal diffusion. Phys Rev 81(5):844–848
33. Dutrieux JF, Platten JK, Chavepeyer G, Bou-Ali MM (2002) On the measurement of positive Soret coefficients. J Phys Chem B 106:6104–6114
34. Bou-Ali MM, Ecenarro O, Madariaga JA, Santamaria C, Valencia JJ (1998) Thermogravitational measurement of the Soret coefficient of liquid mixtures. J Phys: Condens Matter 10:3321
35. Bou-Ali MM, Ecenarro O, Madariaga JA, Santamaria C, Valencia JJ (1999) Soret coefficient of some binary liquid mixtures. J Non-Equilib Thermodyn 24:228
36. Bou-Ali MM, Valencia JJ, Madariaga JA, Santamaria C, Ecenarro O, Dutrieux JF (2003) Determination of the thermodiffusion coefficient in three binary organic liquid mixtures by the thermo-gravitational method (contribution of the Universidad del País Vasco, Bilbao, to the benchmark test), Philos Mag 83:2011
37. Furry WH, Jones RC, Onsager L (1939) On the theory of isotope separation by thermal diffusion. Phys Rev 55:1083
38. Valencia JJ, Bou-Ali MM, Ecenarro O, Madariaga JA, Santamaria C (2002) Validity limits of the FJO thermogravitational column technique. In: Köhler W, Wiegand S (eds) Thermal nonequilibrium phenomena in fluid mixtures, vol 233. Springer, Heidelberg
39. Ecenarro O, Madariaga JA, Navarro JL, Santamaria CM, Carrion JA, Saviron JM (1993) Thermo-gravitational separation and the thermal diffusion factor near critical points in binary liquid mixtures. J Phys: Condens Matter 5:2289
40. Bou-Ali MM, Platten JK (2005) Metrology of the thermodiffusion coefficients in a ternary system. J Non-Equilib Thermodyn 30:385
41. Leahy-Dios A, Bou-Ali MM, Platten JK, Firoozabadi A (2005) Measurements of molecular- and thermal-diffusion coefficient in ternary mixtures. J Chem Phys 122:234501
42. Blanco P, Bou-Ali MM, Platten JK, Alonso de Mezquia D, Madariaga JA, Santamaría C (2010) Thermal diffusion coefficients of binary and ternary hydrocarbon mixtures. J Chem Phys 132:114506
43. Alonso de Mezquia D, Wang Z, Lapeira E, Klein M, Wiegand S, Bou-Ali MM (2014b) Thermodiffusion, molecular diffusion and Soret coefficient of binary and ternary mixtures on n-hexane, n-dodecane and toluene. Eur Phys J E 37:106
44. Costesèque P, Fargue D, Jamet P (2002) Thermodiffusion in porous media and its consequences. In: Köhler W, Wiegand S (eds) Thermal nonequilibrium phenomena in fluid mixtures, vol 389. Springer, Heidelberg
45. Costesèque P, Loubet J-C (2003) Measuring the Soret coefficient of binary hydrocarbon mixtures in packed thermo-gravitational columns (contribution of Toulouse University to the benchmark test). Philos Mag 83:2017
46. Segre PN, Gammon RW, Sengers JV (1993) Light-scattering measurements of non-equilibrium fluctuations in a liquid mixture. Phys Rev E 47:1026
47. Ortiz de Zárate JM, Sengers JV (2006) Hydrodynamic fluctuations in fluids and fluid mixtures. Elsevier, Amsterdam
48. Croccolo F, Ortiz de Zárate JM, Sengers JV (2016) Non-local fluctuation phenomena in liquids. Eur Phys J E 39:125

49. Vailati A, Giglio M (1996) q Divergence of non-equilibrium fluctuations and its gravity-induced frustration in a temperature stressed liquid mixture. Phys Rev Lett 77:1484
50. Vailati A, Cerbino R, Mazzoni S, Takacs CJ, Cannell DS, Giglio M (2011) Fractal fronts of diffusion in microgravity. Nat Commun 2:290
51. Ortiz de Zárate JM, Cordon RP, Sengers JV (2001) Finite-size effects on fluctuations in a fluid out of thermal equilibrium. Phys A 291:113
52. Croccolo F, Bataller H, Scheffold F (2012) A light scattering study of non-equilibrium fluctuations in liquid mixtures to measure the Soret and mass diffusion coefficient. J Chem Phys 137:234202
53. Ortiz de Zárate JM, Giraudet C, Bataller H, Croccolo F (2014) Non-equilibrium fluctuations induced by the Soret effect in a ternary mixture. Eur Phys J E 37:77
54. Bataller H, Giraudet C, Croccolo F, Ortiz de Zárate JM (2016) Analysis of non-equilibrium fluctuations in a ternary liquid mixture. Micrograv Sci Technol 28:611
55. Martinez Pancorbo P, Ortiz de Zárate JM, Bataller H, Croccolo F (2016) Gravity effects on Soret-induced nonequilibrium fluctuations in ternary mixtures. Eur Phys J E
56. Croccolo F, Bataller H (2016) Microgravity in a thin film: how confinement kills gravity. Eur Phys J E 39:132
57. McCourt FRW, Beenakker JJM, Köhler WE, Kuscer I (1990) Non-equilibrium phenomena in polyatomic gases, vol 1. Clarendon Press, Oxford
58. Chapman S, Cowling TG (1991) The mathematical theory of non-uniform gases, 3rd edn. Cambridge Mathematical Library
59. Galliero G, Duguay B, Caltagirone JP, Montel F (2003) On thermal diffusion in binary and ternary mixtures by non-equilibrium molecular dynamics. Phil Mag 83:2097–2108
60. Enskog D (1922) Kungliga Svenska Vetenskapsakademiens. Handlingar 63:5
61. Galliero G, Bugel M, Duguay B, Montel F (2007) Mass effect on thermodiffusion using molecular dynamics. J Non-Equi Thermodyn 32:251–258
62. Villain-Guillot S, Würger A (2011) Thermal diffusion in a binary liquid due to rectified molecular fluctuations. Phys Rev E 83:030501
63. Firoozabadi A, Ghorayeb K, Shukla K (2000) Theoretical model of thermal diffusion factors in multicomponent mixtures. AIChE J 46:892–900
64. Artola PA, Rousseau B, Galliero G (2008) A new model for thermal diffusion, kinetic approach. J Am Chem Soc 130:10963
65. Morozov KI (2009) Soret effect in molecular mixtures. Phys Rev E 79:031204
66. Würger A (2014) Thermodiffusion in binary liquids: the role of irreversibility. J Cond Matt 26:035105
67. Alonso de Mezquia D, Bou-Ali MM, Madariaga JA, Santamaria C (2014) Mass effect on the Soret coefficient in n-alkane mixtures. J Chem Phys 140:084503
68. Gonzalez-Bagnoli MG, Shapiro AA, Stenby EH (2003) Evaluation of the thermodynamic models for the thermal diffusion factor. Phil Mag 83:2171
69. Galliero G, Montel F (2008) Nonisothermal gravitational segregation by molecular dynamics simulations. Phys Rev E 78:041203
70. Artola PA, Rousseau B (2015) Isotopic effect in ternary mixtures, theoretical predictions and molecular simulations. J Chem Phys 143:174503
71. Hafskjold B, Ikeshoji T, Ratkje SK (1993) On the molecular mechanism of thermal diffusion in liquids. Mol Phys 80:1389–1412
72. Rieth D, Müller-Plathe F (2000) On the nature of thermal diffusion in binary Lennard-Jones liquids. J Chem Phys 112:2436–2443
73. Vogelsang R, Hoheisel C (1988) The Dufour and Soret coefficients of isotopic mixtures from equilibrium molecular dynamics calculations. J Chem Phys 89:1588–1591
74. MacGowan D, Evans DJ (1986) Heat and matter transport in binary liquid mixtures. Phys Rev A 34:2133–2142
75. Sarman S, Evans DJ (1992) Heat flow and mass diffusion in binary Lennard-Jones mixtures. Phys Rev A 45:2370–2379

76. Paolini GV, Ciccotti G (1987) Cross thermotransport in liquid mixtures by nonequilibrium molecular dynamics. Phys Rev A 35:5156–5166
77. Simon J-M, Dysthe DK, Fuchs AH, Rousseau B (1998) Thermal diffusion in alkane binary mixtures: a molecular dynamics approach. Fluid Phase Equilib 150–151:151
78. Antoun S, Saghir MZ, Srinivasan S (2018) An improved molecular dynamics algorithm to study thermodiffusion in binary hydrocarbon mixtures. J Chem Phys 148:104507
79. Perronace A, Leppla C, Leroy F, Rousseau B, Wiegand S (2002) Soret and mass diffusion measurements and molecular dynamics simulations of n-pentane–n-decane mixtures. J Chem Phys 116(9):3718
80. Zhang M, Müller-Plathe F (2005) Reverse nonequilibirum molecular-dynaùics calculation of the Soret coefficient in liquid benzene/cyclohexane mixtures. J Chem Phys 123:124502
81. Polyakov P, Müller-Plathe F, Wiegand S (2008) Reverse nonequilibirum molecular dynamics calculation of the Soret coefficient in liquid heptane/benzene mixtures. J Phys Chem B 112:14999–15004
82. Polyakov P, Rossinsky E, Wiegand S (2009) Study of the soret effect in hydrocarbon chain/aromatic compound mixtures. J Phys Chem B 113:13308–13312
83. Galliero G, Srinivasan S, Saghir MZ (2009) Estimation of thermodiffusion in ternary alkane mixtures using molecular dynamics simulations and an irreversible thermodynamic theory. High Temp – High Press 38:315–328
84. Peng DY, Robinson DB (1976) A new two-constant equation of state. Ind Eng Chem Res 15:59
85. Kramers H, Broeder JJ (1948) Thermal diffusion as a method for the analysis of hydrocarbon oils. Anal Chilica Acta 2:687
86. Hoang H, Delage-Santacreu S, Galliero G (2017) Simultaneous description of equilibirum, interfacail and transport properties of fluids using a Mie chain coarse grained force field. Ind Eng Chem Res 56:9213–9226

454183_1_En_8_Chapter ☑ TYPESET ☐ DISK ☐ LE ☑ CP Disp.:11/5/2019 Pages: 21 Layout: T1-Standard